Reconstructing the Discontinuous and Conformational β1/β 3-Loop Binding Site on hFSH/hCG by Using Highly Constrained Multicyclic Peptides

Smeenk, L.E.J.; Timmers-Parohi, D.; Benschop, J.J.; Puijk, W.C.; Hiemstra, H.; van Maarseveen, J.H.; Timmerman, P.

DOI
10.1002/cbic.201402540

Publication date
2015

Document Version
Final published version

Published in
ChemBioChem

ChemPubSoc Europe

DOI: 10.1002/cbic.201402540

CHEMBIOCHEM Full Papers

VIP

Reconstructing the Discontinuous and Conformational β1/β3-Loop Binding Site on hFSH/hCG by Using Highly Constrained Multicyclic Peptides

Linde E. J. Smeenk,[a] Drohpatie Timmers-Parohi,[b] Joris J. Benschop,[b] Wouter C. Puijk,[b] Henk Hiemstra,[a] Jan H. van Maarseveen,[a] and Peter Timmerman*[a, b]

Making peptide-based molecules that mimic functional interaction sites on proteins remains a challenge in biomedical sciences. Here, we present a robust technology for the covalent assembly of highly constrained and discontinuous binding site mimics, the potential of which is exemplified for structurally complex binding sites on the "Cys-knot" proteins hFSH and hCG. Peptidic structures were assembled by $Ar(CH_2Br)_2$-promoted peptide cyclizations, combined with oxime ligation and disulfide formation. The technology allows unprotected side chain groups and is applicable to peptides of different lengths and nature. A tetracyclic FSH mimic was constructed, showing >600-fold improved binding compared to linear or monocyclic controls. Binding of a tricyclic hCG mimic to anti-hCG mAb 8G5 was identical to hCG itself (IC_{50} = 260 vs. 470 pM), whereas this mimic displayed an IC_{50} value of 149 nM for mAb 3468, an hCG-neutralizing antibody with undetectable binding to either linear or monocyclic controls.

Introduction

The majority of protein–protein interaction sites (PPIs) is discontinuous and/or conformational in nature,[1–8] where residues remote in the primary sequence latch onto each other and constitute a constrained binding site that is only functional when organized in the right manner. The ability to rebuild such binding sites with synthetic peptides is a major challenge in the field. When available, such mimics have great potential for antagonizing PPIs, or as immunogens for generating monoclonal antibodies (mAbs) against difficult-to-target protein targets (e.g., 7TM membrane receptors, ion channels, or β-barrel proteins). Alternatively, they could provide the basic constituent of a prophylactic or therapeutic vaccine formulation for the treatment of target-driven diseases.[9–12]

So far, most research in protein binding site mimicry has focused on maximizing the α-helical or β-turn content of a single peptide to improve its therapeutic potency.[13–16] Despite great achievements, this approach is often insufficient, and different strategies, such as the construction of discontinuous peptide mimics,[17] are desperately needed. Early work by Mutter introduced the TASP[18] and RAFT[19,20] platforms for the assembly of multiple α-helix bundles. Also, other platforms (e.g., steroids,[21] calix[4]arenes,[22] and carbohydrates[23]) were developed for mounting two,[24] three,[25] or four[20,26] different peptide fragments onto a synthetic platform.

Notwithstanding synthetic elegance, most of these strategies involve overly complex (orthogonal) protection/deprotection strategies (use of Boc, Fmoc, Alloc, oNBS, Dde, etc.) that severely limit their general utility. Supramolecular scaffolds elegantly circumvent this problem[27] but lack practical utility because they are limited to the formation of fully symmetric assemblies. Quite recently, a novel rationally-designed coiled-coil α-helical protein scaffold named "alphabodies" for the mimicry of discontinuous epitopes was launched.[28] Here, we describe a novel synthetic methodology for the simple and straightforward assembly of tri- and tetracyclic peptide mimics of the discontinuous β1/β3-loop epitopes on human follicle stimulating hormone (hFSH)[29] (Figure 1A, B) and human chorionic gonadotropin (hCG)[30] (Figure 1C, D), two members of the glycoprotein hormone family.[31] Both hFSH and hCG are heterodimers consisting of a hormone-aspecific α-subunit (identical for hFSH and hCG) and a hormone-specific β-subunit.[31] Key to the technology is that all chemical conversions (i.e., cyclization *and* ligation) proceed in aqueous solutions (>75% H_2O) and are fully compatible with side-chain-unprotected peptides, thus alleviating the need for tedious side-chain protection–deprotection strategies.[25] Moreover, the $Ar(CH_2Br)_2$-promoted peptide cyclization proceeds at a very low concentration (~100 μM) and under mild conditions (25 °C, pH 7.8, no catalyst) but still reaches completion in less than an hour. The technology is applicable to peptides in solution as well as on solid-phase, enabling it to be applied to surface-immobilized arrays of peptides. The resulting protein mimics are readily soluble in water and can be easily assayed by using standard biochemical analyses, like ELISA. We demonstrate the

[a] Dr. L. E. J. Smeenk, Prof. Dr. H. Hiemstra, Dr. J. H. van Maarseveen, Prof. Dr. P. Timmerman
Van't Hoff Institute for Molecular Sciences, University of Amsterdam
Science Park 904, 1098 XH Amsterdam (Netherlands)
E-mail: peter.timmerman@uva.nl

[b] D. Timmers-Parohi, Dr. J. J. Benschop, W. C. Puijk, Prof. Dr. P. Timmerman
Pepscan Therapeutics
Zuidersluisweg 2, 8243 Lelystad (Netherlands)

Supporting information for this article is available on the WWW under http://dx.doi.org/10.1002/cbic.201402540.

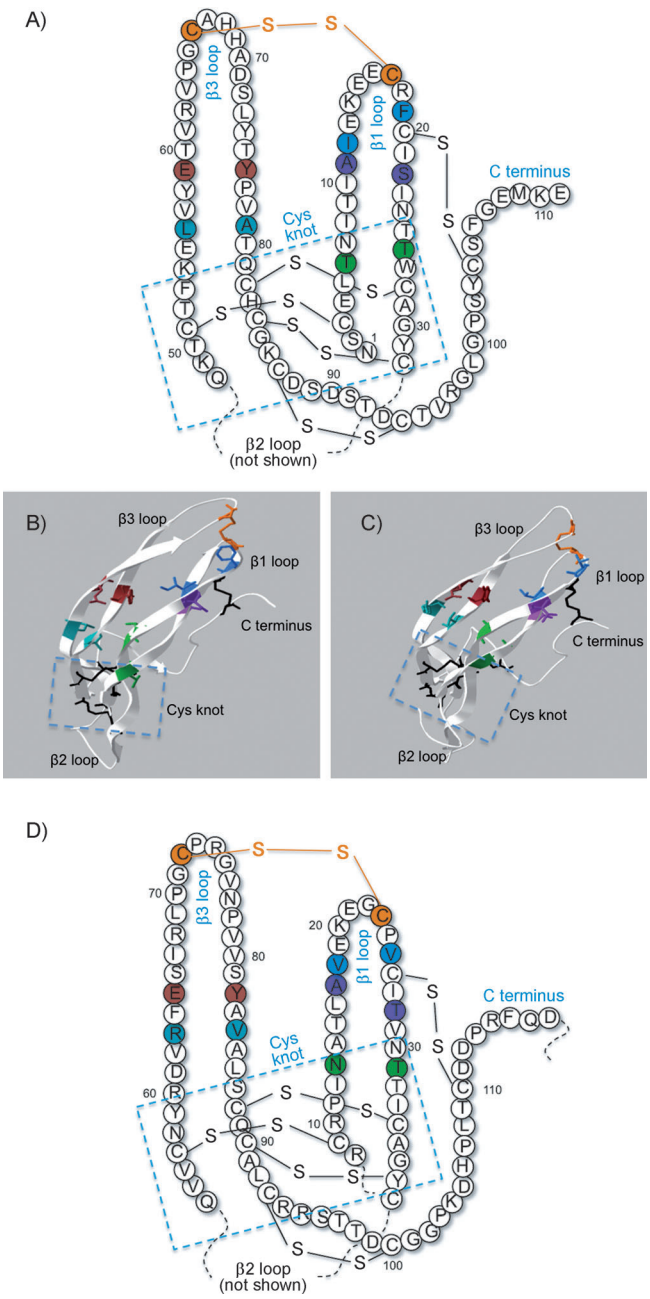

Figure 1. Schematic representation of the folded β-subunit of hFSH (A) and hCG (D) and corresponding X-ray structures[29,30] (B and C from PDB IDs: 1XWD and 1HRP, respectively). The native disulfide bridge linking the β1 and β3 loops is represented in orange. The amino acids that were substituted by cysteines for attachment of the synthetic scaffolds are indicated in green, purple, blue, brown, and turquoise.

strongly enhanced binding properties towards a series of four neutralizing mAbs that apparently do recognize discontinuous epitopes on these proteins (mAbs 5828/6602 for FSH;[32] mAbs 4F9/8G5/3468 for hCG[33]), particularly when these mimics are compared to their linear or "unfolded" reference peptides. The size of these constructs is between 3–6.5 kDa, which is roughly five to ten times smaller than the parent proteins hCG and hFSH.

This new technology builds on earlier work with double-constrained peptides covering the β3-loop epitope on hFSH ($hFSH_{56-79}$), which has already generated antisera with strongly improved neutralizing activities as compared to either linear or single-constrained variants.[34]

Results and Discussion

Synthesis of tri- and tetracyclic hFSH/hCG mimics I–V

The synthesis of tri- and tetracyclic hFSH and hCG mimics was achieved through a tandem "cyclization–ligation" reaction of linear peptides (derived from the β1/β3-loop region in hFSH or hCG), as shown in Figure 2A (for details, see Table S1 in the Supporting Information). Cyclization was performed with either scaffold oS2-NH_2 or oS2-CH=O. During this conversion, one of the terminal cysteines in the peptide reacts with one of the benzylic bromide functionalities of the scaffold to form the linear 1:1 "peptide–oS2" adduct, which instantaneously cyclizes through reaction of the remaining cysteine and benzylic bromide functionality to give the corresponding single-loop CLIPS peptide in very good to excellent yields (60–90%, Table S2). Removal of the acid-labile protecting groups (ONHBoc for oS2-NH_2, $CH(OEt)_2$ for oS2-CH=O) was achieved by TFA-treatment in MeCN/H_2O (for oS2-CH=O) or in CH_2Cl_2 (for oS2-NH_2). Coupling of the deprotected single-loop β1 and β3 mimics to give the corresponding discontinuous β1/β3 mimics was achieved with >95% conversion (Tables S3 and S4) by using the aniline-catalyzed oxime ligation reaction as described by Dawson.[35]

The oxime ligation was the only reaction that could successfully be performed when using stoichiometric amounts of the reacting peptides and explicitly did not require one of these to be used in large excess. The ligation reaction proceeded smoothly and cleanly within 30 min at room temperature at the typical concentrations of 100–500 μM that are usually required for efficient manipulation of 2–5 kDa peptides. In this respect, many of the other ligation reactions (i.e., CLICK, thiol-ene) failed, as conversion to the bicycle peptides could only be achieved when using large excesses of one of the reactants. The final step in the construction of tricyclic FSH and hCG mimics **I**–**IV** was the formation of a disulfide bond between the β1 and β3 loops, which is also present in the parent proteins (C_{17}–C_{66} in hFSH; C_{23}–C_{72} in hCG). This was achieved by treatment with excess I_2 in MeOH to remove the Acm protecting groups at the cysteines, followed by treatment with excess 1,4-DTT to fully reduce the liberated thiol groups. Then, the peptides were reoxidized in air at high dilution (1 mg mL^{-1}) in Tris·HCl buffer (pH 8.0) for three days at room temperature to ensure the clean and exclusive formation of *intra*molecular disulfide bonds in **I** (Table S5 and Figure S1). This finally gave rise to a set of four hFSH mimics (**Ia**–**c**, **IIIa**), four hCG mimics (**IIa**–**b**, **IVa**–**b**), and corresponding controls (**1**–**7**, Figure 2B, C; for details on synthesis, see the Supporting Information). Besides these, a variety of related β1/β3-loop mimics were fabricated by using the trifunctional scaffold 1,3,5-tribromomesitylene. However, none of these showed measurable binding activity to the mAbs investigated, which is likely attributed to sub-optimal fixation of the peptide loops.

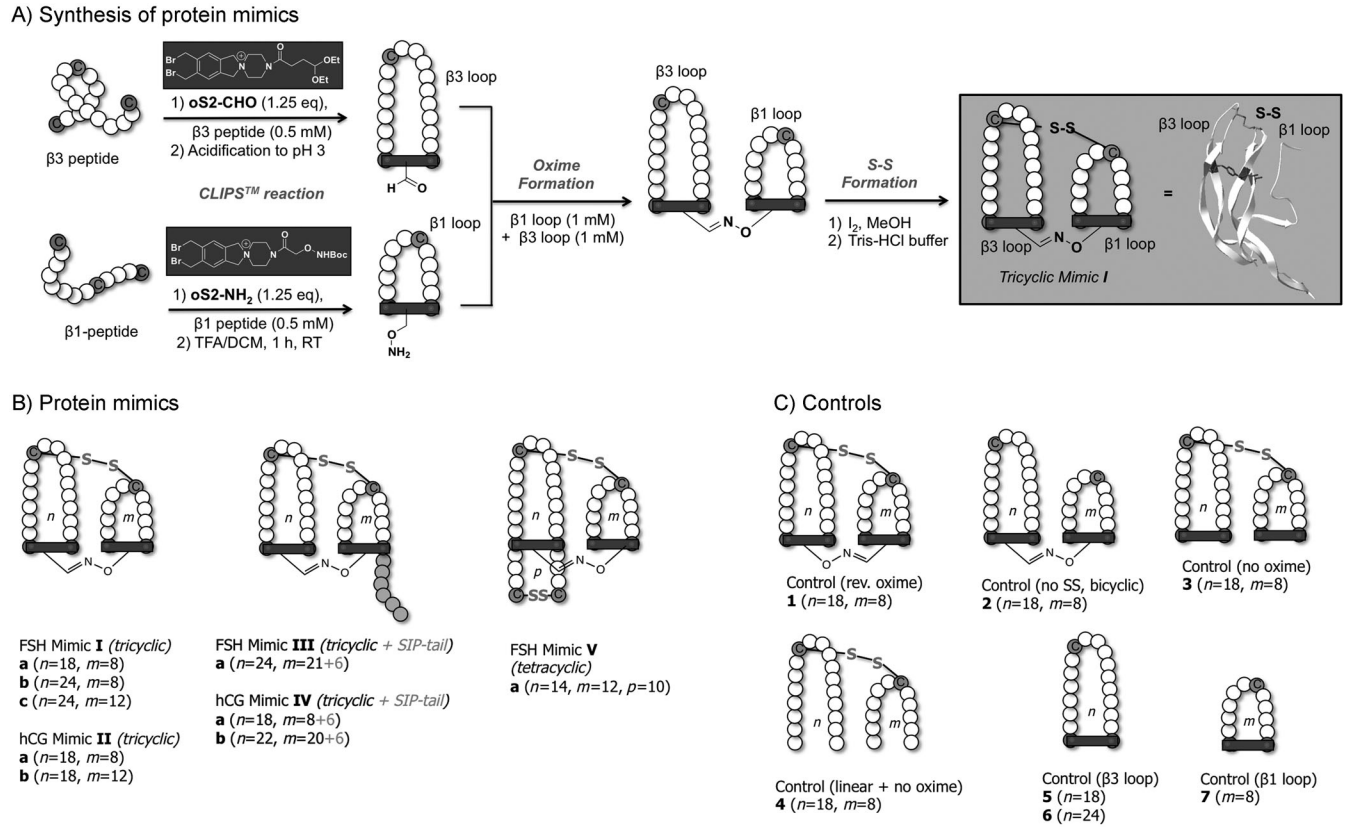

Figure 2. A) General concept of hFSH and hCG mimic synthesis. Linear β1 or β3 peptides (derived from hFSH or hCG) were cyclized by reaction with either scaffold oS2-CH=O or oS2-NH_2. Subsequently, oxime ligation of the β1- and β3-loop peptides was performed, forming a bicyclic β1/β3-loop mimic. Finally, disulfide bond formation was achieved by means of Acm protecting group removal, followed by re-oxidization of the peptides in air to give the tricyclic mimics **I**. B) Schematic representation of the hFSH and hCG protein mimics. C) Schematic representation of the hFSH and hCG relevant controls. Peptide lengths (*n*, *m*, and *p*) are given for each compound.

We also synthesized tetracyclic mimic **V** (Figure 2B), in which an additional disulfide bond is present between the N and C termini of the β3 loop. This increased the structural rigidity of this loop and significantly improved its binding potential (vide infra). Design and synthesis of **V** largely parallels that of mimics **I**–**IV**, with the difference that the extra Cys(Acm) groups located at the termini of the β3 loop get removed together with the other Cys(Acm) groups during the oxidative deprotection step (vide supra). Upon reoxidation in folding buffer (Figure S1), the four liberated thiols simultaneously form two disulfide bonds in a fully selective manner, as judged by the appearance of a single peak in the UPLC/UV spectrum. Supposedly, the four thiols are highly pre-organized as to preferably form a disulfide bond with their nearest neighbor, as this will give rise to the thermodynamically most stable isomer.

As the increased hydrophobicity of the longer β1 loops ($m >$ 12) in mimics **I** and **II** severely limited their water solubility, it was decided to introduce a Lys_6 chain ("SIP-tail") at the C-terminal end of these peptides (mimics **III** and **IV**).[36] As expected, this greatly improved the overall quality of the linear β1 peptides, as well as the ease of manipulation and the overall solubility of the β1/β3-loop constructs in water.

Binding analysis of tri- and tetracyclic FSH mimics I, III, and V to anti-hFSH mAbs 5828 and 6602 by ELISA

In order to verify the potential of tricycle mimic **I** to act as real mimics of the structurally complex β1/β3-loop epitope on hFSH and hCG, we studied their binding strength to two anti-hFSH monoclonal antibodies, that is, mAb 5828 and 6602, by ELISA. These mAbs displayed the strongest FSH-neutralizing activity from a panel of ~40 different mAbs and were previously mapped to bind to the discontinuous β1/β3-loop epitope.[32] hFSH mimic **Ia** and controls **1**–**7**, together with the hFSH protein itself, were surface-immobilized and subsequently tested for mAb binding over a wide concentration range (5000–0.1 ng mL^{-1}) in the presence of diluted horse serum (5%) and ovalbumine (4%) as blocking reagents, the results of which are given in Figure 3.

Both mAbs 5828 and 6602 bound strongly to tricyclic mimic **Ia**, with EC_{50} values comparable to those for the hFSH protein itself (54 and 48 ng mL^{-1} for **Ia**, and 14 and 29 ng mL^{-1} for hFSH). The orientation of the oxime linkage was found to be irrelevant for mAb binding, as both mimic **Ia** (normal oxime) and control **1** (reversed oxime) bound equally well to both mAbs (EC_{50} = 54/59 and 48/98 ng mL^{-1}, respectively). However, presence of the native S–S bond at C_{17}–C_{66}, connecting the β1

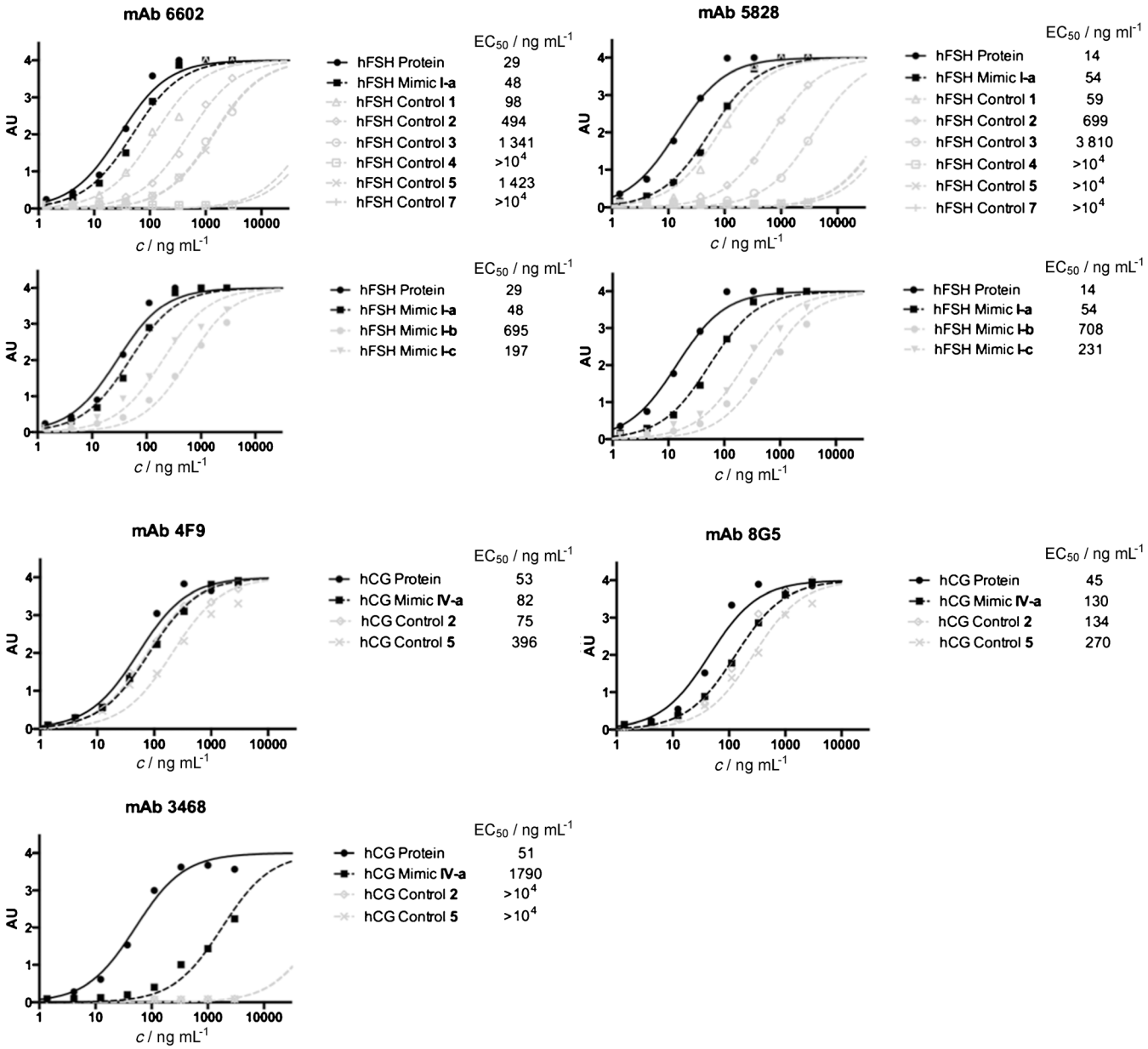

Figure 3. Antibody binding curves measured by ELISA. The hFSH and hCG mimics were immobilized onto the plate surface by using GDA coating. The plates were incubated with mAbs 6602/5828/3468/8G5/4F9 at eight different dilutions, starting at 3.0 $\mu g\,mL^{-1}$ in the first well and threefold dilutions in subsequent wells. Incubation was performed for 1 h at 37 °C.

and β3 loops in hFSH, was highly relevant, as binding of bicyclic control **2** was approximately ten times lower (EC_{50} = 699 and 494 $ng\,mL^{-1}$ for both mAbs). Additional release of constraints, as for controls **3**–**7**, further reduced mAb binding. For example, control **3**, which lacks the oxime linkage but has an intact S–S bond at C_{17}–C_{66}, showed severely weakened binding (EC_{50} = 3810 and 1341 $ng\,mL^{-1}$ for both mAbs). Furthermore, control **4**, which lacks both the oxime linkage and the CH_2-Ar-CH_2 constraints, while having an intact S–S bond at C_{17}–C_{66}, showed no binding at all (EC_{50} > 10000 $ng\,mL^{-1}$ for both mAbs). Binding of the monocyclic controls **5** and **7** was undetectable for mAb 5828, even at the highest possible concentration (5 $\mu g\,mL^{-1}$), whereas only weak binding to the β3 loop of **5** was observed for mAb 6602 (EC_{50} = 1423 $ng\,mL^{-1}$).

Binding of mAbs 5828 and 6602 to tri- and tetracyclic hFSH mimics **I**, **III**, and **V** was then investigated in solution by using a competition ELISA setup. In such an experiment, the ability of the mimics (and controls) to block binding of the mAbs to surface-immobilized hFSH mimic **Ia** was tested at various concentrations, with hFSH as a reference compound (Figure 4). Inhibition of mAb binding was clearly observed for all three tricyclic mimics (**Ia**–**c**), with IC_{50} values in the ~10–90 μM range (Figure 4), whereas hFSH itself competed at much lower concentrations (IC_{50} = 0.17 and 0.27 nM). In contrast, the single-β3-loop controls (**5** and **6**) did not show measurable inhibition below a concentration of 100 μM. The tricyclic mimic **Ic**, with elongated β1 and β3 loops (m = 12, n = 24; IC_{50} = 13.8 and 9.5 μM) was clearly more active than mimic **Ia**, which has much

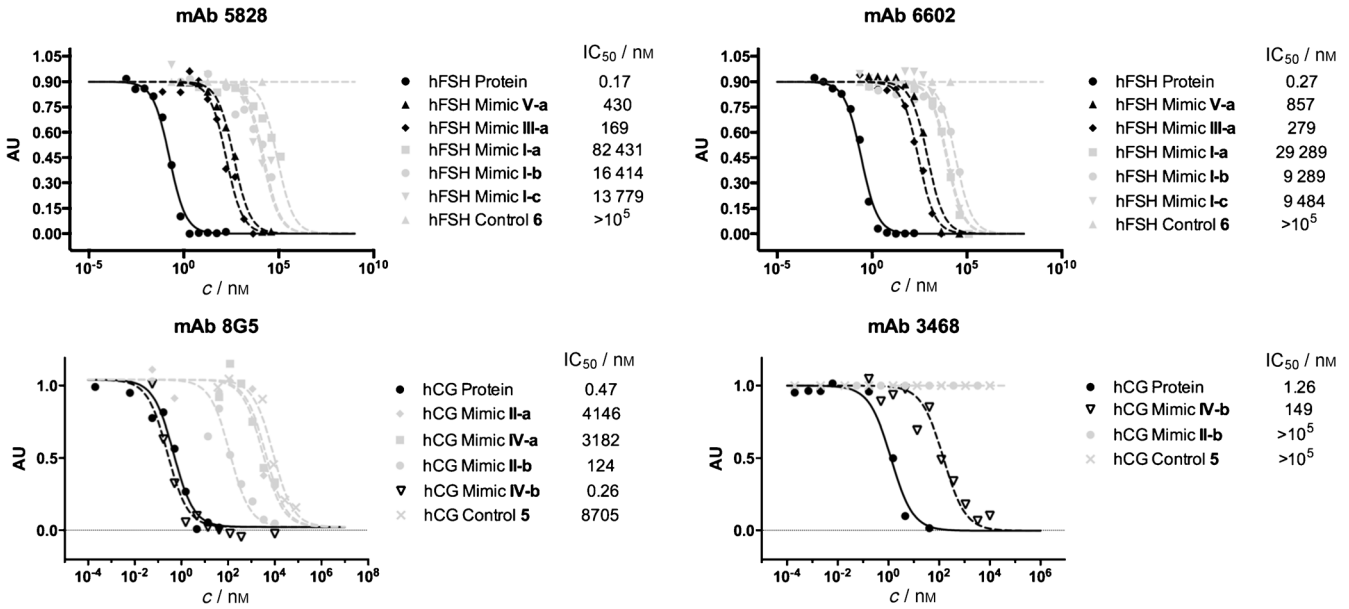

Figure 4. Antibody binding competition curves measured by ELISA. Antibodies were pre-incubated with the hFSH/hCG mimics for 30 min at 37 °C in a separate pre-incubation plate, followed by incubating the combined solutions in a protein- or protein-mimic-coated ELISA plate for 1 h at 37 °C. In this way, the concentration of mimics (IC_{50}) at which mAb binding was reduced to 50% of the original value (without the mimics present) was determined. mAb concentrations that gave an $OD_{405\,nm}$ value of 1.0–1.5 A.U. in binding ELISA experiments were found to give optimal results in the competition experiments.

shorter loops ($m=8$, $n=18$, $IC_{50}=82.4$ and 29.3 μM). We also observed that introduction of the solubility-inducing SIP-tail (Lys_6 sequence) in tricyclic mimic **Ic** (which gives mimic **IIIa**) significantly lowered the concentration at which mAb binding to the ELISA surface was inhibited ($IC_{50}=169$ and 279 nM for both mAbs). Interestingly, the tetracyclic mimic **Va**, having an extra S–S constraint at the bottom of the β3 loop (see Figure 2B), showed a substantial enhancement in inhibitory activity for both mAbs ($IC_{50}=430$ and 857 nM), which is equivalent to a ten- to 30-fold increase in comparison to the triple-constrained FSH mimic **Ic**. The extra covalent S–S linkage was intended to better support the β-hairpin structure of the β3 loop in **Va**, thus preorganizing the overall shape for improved binding to the mAbs.

Binding analysis of tricyclic hCG mimics II and IV to anti-hCG mAbs 4F9, 8G5, and 3468

Next, we determined binding of the tricyclic hCG mimics **II** and **IV** (and controls) to a panel of three different anti-hCG mAbs by ELISA. Of these, mAb 3468 was characterized by X-ray crystallography (PDB ID: 1QFW) to bind to a highly conformational and discontinuous binding site located at the top of the β3 loop of hCGβ, with clear involvement of the β1 loop by means of the side chain of Lys20 (Figure 5).[33] Moreover, the β1 loop seems to provide structural support for the β3 loop by means of multiple interactions between the hydrophobic side chains of Leu16, Val18, Ile27, Val29, and Thr31, represented as orange residues in Figure 5. We determined that a maximum of 4–5 hCGβ residues (Lys20, Phe64, Arg74, Val79, Ser81) make direct contact with mAb 3468, whereas at least eight to ten residues are involved in structuring the loops for binding.

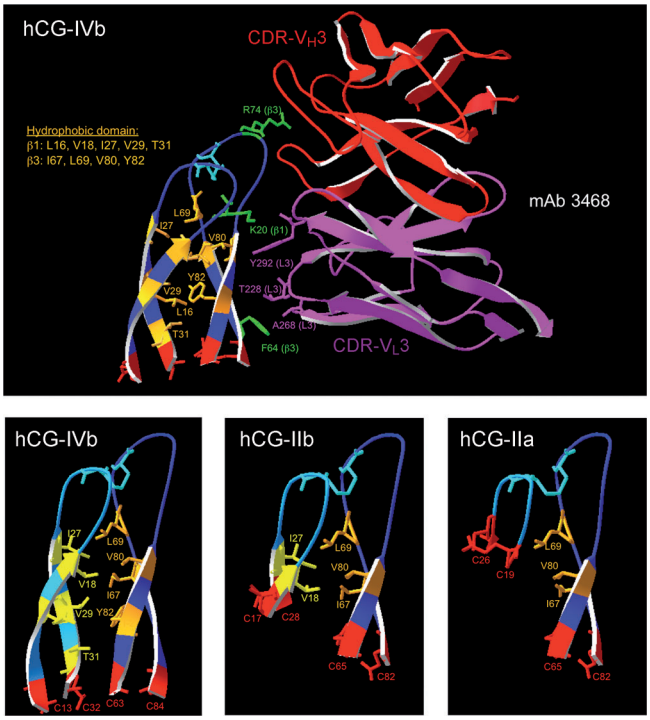

Figure 5. X-ray crystal structure of the hCGβ·mAb 3468 complex (PDB ID: 1QFW), illustrating the molecular organization of the discontinuous β1-/β3-loop binding site of mAb 3468 on hCG and showing the orientation of important side chains (green) on hCG (e.g., Lys20, Arg74, Phe62) interacting with mAb 3468 (PDB ID: 1QFW). The structural organization of the sequences that correspond to tricyclic mimics **IIa**, **IIb**, and **IVb** illustrates how the absence (e.g., **IIa**) and presence of the hydrophobic folding domain (orange) preorganizes the β1 and β3 loops for binding.

It is therefore likely that the presence of the β1-loop sequence, when long enough, will significantly strengthen binding of a single β3 loop to mAb 3468. For mAbs 4F9 and 8G5, previous binding experiments with linear β3-loop peptides in ELISA provided clear evidence for a β3-loop epitope,[37] but information other than that was not available. We observed that all three mAbs showed strong binding to tricyclic hCG mimic **IVa** by ELISA (Figure 3), virtually identical to that of hCG (less than twofold difference).

The profiles for mAbs 4F9 and 8G5 were very similar, with equally strong binding for hCG and mono-, bi-, and tricyclic mimics (< 3.5-fold difference), and presumably little to no involvement of the β1 loop. In contrast, mAb 3468 showed no detectable binding to monocyclic β3-loop controls (Figure 3). Incorporation of the β1 loop and S–S bond, as in **IVa**, considerably enhanced mAb binding (EC_{50} = 1296 and 1790 ng mL^{-1} for mAb 3468).

The ability of hCG mimics **II** or **IV** (and controls) to block the binding of mAbs 8G5 and 3468 to surface-immobilized hCG was then determined in a competition ELISA experiment (Figure 4). Again, most of the mimics showed much weaker binding in solution than when immobilized to the ELISA surface, similar to what was observed for the hFSH mimics. For example, mAb 8G5 showed an 8800-fold lower binding activity to tricyclic mimic **IIa** in solution than to hCG (IC_{50} = 4146 vs. 0.47 nM for hCG), whereas the same mAb bound with almost equal strength to surface-immobilized **IIa** and hCG in ELISA (EC_{50} = 130 vs. 45 ng mL^{-1}, respectively). Much to our surprise, mimic binding of mAb 8G5 in solution was strongly improved when elongating the sequence of both the β1- and β3 loops. In fact, by extending the β1 loop of mimic **IIa** by four amino acids (from octa- to 12-mer) the binding of mAb 8G5 improved by a factor of ~33 (IC_{50} value of 4146 nM for **IIa** and 124 nM for **IIb**). Binding of 8G5 was even further improved (475-fold) upon additional extension of both the β3 loop (from 18- to 22-mer) and the β1 loop (from 12- to 20-mer), with an IC_{50} value of 0.26 nM for mimic **IVb**, fully identical to that of hCG itself (IC_{50} = 0.47 nM). In order to rule out the possibility that the solubility-improving Lys_6 tail in **IVb** was responsible for the observed activity improvements, the same tail was introduced into mimic **IIa** (resulting in mimic **IVa**) and did not change the binding activity to mAb 8G5 (IC_{50} = 3.2 and 4.1 μM for mimics **IIa** and **IVa**, respectively).

Evaluation of mAb 3468 binding to tricyclic mimics **II** and **IV** in solution clearly revealed this to be the most challenging of all mAbs investigated. Binding of this mAb to tricyclic mimic **IVa** was completely undetectable below 10 μM in solution, whereas binding of mAb 3468 to mimic **IVa** when immobilized to the ELISA surface was basically identical to that of hCG (EC_{50} = 78 vs. 51 ng mL^{-1} for mimic **IVa** and hCG, respectively). For mAb 3468, we also observed that elongation of both the β1 and β3 loop (from 18- to 22-mer for β1 loop and from 12- to 20-mer for β3 loop), as in mimic **IVb**, was sufficient to improve the binding of this mAb by at least 67-fold, to IC_{50} = 149 nM, which is only about 100 times lower than for hCG itself.

Binding analysis of tricyclic hFSH and hCG mimics I and II by using arrays of overlapping peptides

Subsequently, we investigated the contribution of the β1 loop to mAb binding in mimics **I** and **II** to the single amino acid level by using Pepscan peptide arrays.[38] The mimics were immobilized on the array surface via the C-terminal end of their β1 loops and then assembled in a stepwise manner by using identical procedures to those in solution. First, we synthesized overlapping libraries of peptides of varying lengths [Ac-C(X)$_n$C–linker–surface; n = 6, 8, 10, 12] that were all derived from the β1-loop domain of hFSH (residues 8–27). Subsequently, each peptide in the library was cyclized by using scaffold oS2-NH_2 and then oxime ligated to the cyclic β3 loop (C_TTVRVPGC-(Acm)AHHADSLYTC_T) that was cyclized by using the complementary scaffold oS2-CH=O. Finally, the β1 and β3 loops were S–S-bonded by oxidative deprotection of the Acm protecting groups on the native cysteines (Cys17/Cys66) (total of 28 tricyclic mimics **I** and 60 bicyclic controls **2**). For comparison, the same library without the native S–S bond was also synthesized. Binding of mAb 6602 and 5828 to the tricyclic mimics (type **I**) was greatly improved as compared to the corresponding single β1- and β3-loop control sequences (OD_{405nm} ~2.0 vs. < 0.1 A.U. at 100 ng mL^{-1}, see Figures 6A and S3 for the complete scan). mAb binding was not observed for all mimics in the library but only for those covering the top of the β1 loop (i.e., including the sequence ^{13}EKEE^{16}). Binding was twice as strong for tricyclic mimics **I** as for the bicyclic controls **2** without the native S–S bond, but equal to binding of tricyclic controls with a reversed oxime linkage (controls **1**). We also established that mAb binding was clearly correlated to the native sequence of the β1 loop, as binding of two scrambled variants of the β1-loop sequence showed strongly reduced binding (four- and sevenfold decrease for mAbs 5828 and 6602, respectively).

Next, a complete amino acid replacement analysis of the β1 loop for the strongest binding mimic **I** ([C_{oS2}TVRVPGC_{SS}AHHAD-SLYTC_{oS2}]-oS2-CH=N-O-oS2-[C_{oS2}IEKEEC$_{SS}$RFAIC_{oS2}]; Figure 6B) was carried out. It revealed the essential role of only a single β1-loop residue, that is, Lys14, for both mAb 6602 and 5828 binding (Figure 6B, C).

Previously, a similar replacement study for the β3 loop revealed the essential role of residues Arg61, Gly65, Asp72, and Leu74 for binding, which are all in the same subdomain as Lys14 in the folded structure of FSH.[29,39] Replacement of Lys14 by any other amino acid, including arginine, inhibited binding almost completely (green squares in Figure 6C). The fact that the basic amino acid arginine also cannot replace Lys14 well excludes the possibility that the observed effect is due to a nonspecific surface-charge effect.[40] The three Glu residues flanking Lys14 also seem to be involved in the binding of mAb 5828, as replacement of these also significantly reduces mAb binding. However, the remaining β1-loop residues do not seem to contribute much to binding (black squares in Figure 6B).

For mAb 6602, Lys14 is the only essential amino acid; the effect of replacement for the other residues is non-systematic

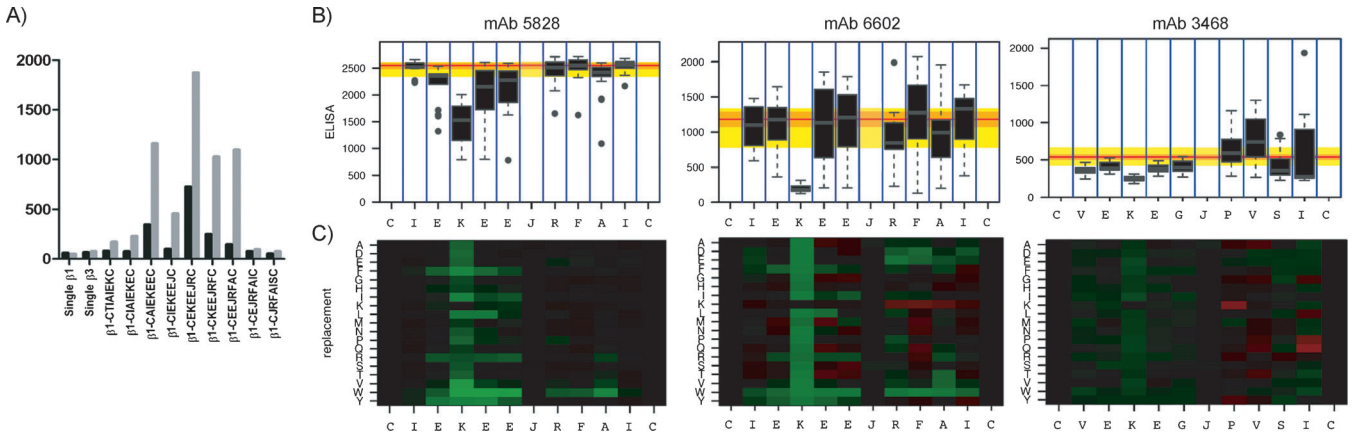

Figure 6. A) OD_{405} for binding of tricyclic mimics **I**, covalently attached to the surface via octamer β1-loop peptides to mAb 5828 (■) and 6602 (■, 100 ng mL^{-1}; results for other β1-loop lengths are given in the Supporting Information). B) Box-plot representation of residue relevance of hFSH and hCG β1-loop sequence (Ac-C_{oS2}IEKEEC$_{SS}$RFAIC$_{oS2}$-NH_2 and Ac-C_{oS2}VEKEGC$_{SS}$PVSIC$_{oS2}$-NH_2, respectively) for binding of mAbs 5828, 6602 (hFSH), and 3468 (hCG). Red, yellow, and black bars indicate, respectively, the average, SEM, and 95% confidence intervals for mAb binding levels of the native peptide mimic. C) Heat map representation of the replacement analysis data; green indicates a decrease in mAb binding, red indicates an increase in mAb binding, and black indicates no change in binding.

(random green/black/red squares). A similar replacement analysis was also performed for tricyclic mimic **II** of hCG ([C_{oS2}SIRLPGC$_{SS}$PRGVNPVVSYAC$_{oS2}$]-oS2-CH=N-O-oS2-[C_{oS2}VEKEGC$_{SS}$PVSIC$_{oS2}$]; Figure 6C). Interestingly, binding of mAb 3468 showed a very similar pattern to anti-FSH mAb 5828, with the sequence ^{18}VEKEG^{22} identified as important for binding and Lys20 being the most essential amino acid. In particular, replacement of the hydrophobic residues that are C-terminal to the native cysteine (Pro24/Val25/Ile27) improved binding, which seems to indicate that these residues freeze the β1 loop in a suboptimal conformation for binding. This seems to be in accordance with the fact that most replacements with Trp, Phe, or Ile influence the binding in a negative manner (also observed for mAbs 5828 and 6602).

Conclusion

We applied our recently developed methodology for cyclization and subsequent ligation of different peptide domains[41] to the manufacturing of a large series of discontinuous β1/β3-loop epitope mimics of hFSHβ and hCGβ. These mimics are monodisperse compounds, some of which exhibit decent functional activities, thanks to 1) very good solubilities in aqueous buffers (even at high concentration) that makes these usable in standard biochemical assays, like ELISA; 2) the synthesis of C_{2v}-symmetric scaffolds that form only a single product upon coupling of intrinsically asymmetric peptides, thereby preventing the formation of complex diastereomeric product mixtures; and 3) setting up reliable and compatible chemistries for cyclization, conjugation, and S–S oxidation that are applicable to peptides of very different nature and provide end products of good quality and purity. The very high reactivities and selectivities observed in CH_2-Ar-CH_2 cyclizations and oxime ligation (< 1.0 mM in aqueous buffers at room temperature, no side-chain-protecting groups) are unique and indispensable for manufacturing these structurally complex protein mimics. Moreover, the Acm deprotection method with I_2 was universally applicable,[42] and worked far better than any of the literature procedures involving heavy metals (Ag^+, Tl^{3+}, or Hg^{2+}).

We observed strong binding of anti-hFSHβ and anti-hCGβ mAbs to tri- and tetracyclic mimics (**I**–**IV**), in some cases even with comparable strength to the native proteins. The joint force of three different chemical constraints—that is, CH_2-Ar-CH_2, oxime linkage, and (native) S–S bond(s)—was found to be crucial for binding, as linear discontinuous controls like **4**, or monocyclic controls like **5** and **6**, showed far lower activities. Apparently, the mere presence of primary protein sequences in the form of flexible S–S-linked peptides imic **4**) is insufficient for mAb binding, and physical constraints that pre-organize the binding functionalities in the correct 3D orientation are required.

The remarkably strong difference in surface (ELISA) and solution (competition) mAb binding is striking and shows that interpreting surface data as being representative for binding in solution leads to the wrong conclusions. The strongest difference was observed for the mimics with the shortest β1 loops ($m = 8$; **Ia**/**IIa**/**IVa**), which are almost inactive in solution while being the strongest binders at the surface. It seems like the ELISA surface supports the scaffolds in their role to structure the peptide constructs for binding. We observed for three of four mAbs that the lysine at the top of the β1 loop (Lys14 for FSHβ; Lys20 for hCGβ) was crucial to binding (Figure 6), but its presence was insufficient to make mimics **Ia**/**IIa**/**IVa** strong binders in solution. In fact, we learned that the lower residues at the β1 and β3 loops also play a crucial role in binding, even though they are unlikely to directly contact the antibodies.

For example, the IC_{50} value for mAb 8G5 was improved from 4146 to 124 nM (factor of ~33) by elongating the β1 loop only with four residues (from octa- to 12-mers). The biggest difference in binding (~16000) of mAb 8G5 was seen for mimics **IIa** (4146 nM), and **IVb** (0.26 nM), which differ only in the length of the β3 (18- vs. 22-mer) and β1 loops (12- vs. 20-mer). The most

likely explanation is that the lower residues in mimic **IVb** constitute a hydrophobic folding domain that fixes the β3 and β1 loops in the correct orientation for optimal mAb binding (see Figure 5). When absent, as in **IIa**, the loops are too disordered and flexible for binding of mAb 8G5.

mAb 3468 showed a similar behavior, but with a much smaller difference (~70-fold) in binding for **IIa/b** ($>10^5$ nM) and **IVb** (149 nM). The X-ray structure also reveals that the lower β3-loop residue Phe64 (only present in **IVb**, not in **IIb**) makes an additional contact with hCG, but this positive interaction will again depend on properly oriented β3 and β1 loops (Figure 5). Finally, the ~200-fold improvement for binding of tetracyclic mimic **V** as compared to tricyclic equivalent **Ic** further supports the importance of the effect of structural fixation to binding. The final ~100-fold difference between binding of the proteins and the best mimics could relate to yet suboptimal structural organization in the mimics but also to atomic contacts of the mAbs to the glycosylated sites at the bottom of the β1 loops (e.g., Asn24/Asn42 in hCG) that are not present in the mimics.

Our findings on the improved bioactivities of tri- and tetracyclic hFSH and hCG mimics correspond well to those of other laboratories,[43] describing bicyclic peptide binders with strongly improved activities as compared to linear and monocyclic controls.

Experimental Section

General procedure for $Ar(CH_2Br)_2$-promoted peptide cyclization reactions. Dithiol-containing peptide (1 equiv) was dissolved in MeCN/H_2O (1:3) to a final solution of 0.5 mM. The scaffold (oS2-ONH_2/oS2-CHO, 1.25 equiv) was added, followed by the addition of 40 equiv Na_2CO_3, to a final pH of 8. The reaction mixture was stirred for 30 min, quenched with 1% TFA until pH 3, and stirred for another 1 h. In the case of scaffold oS2-NH_2, after solvent evaporation in vacuo, the residue was dissolved in TFA/CH_2Cl_2 (1:1) and stirred for 1 h. Direct preparative HPLC purification, followed by freeze-drying, resulted in the final products.

Procedure for oxime ligation. Peptides were dissolved 1:1 in a 100 mM citric acid (21.0 mg mL^{-1})/aniline (9 μL mL^{-1}) buffer to obtain a final solution of 1 mM. The reaction was stirred for 15 min and directly purified by preparative HPLC, followed by freeze drying.

Procedure for Acm removal and disulfide bond formation. Cys(Acm)-containing compound was dissolved in guanidine·HCl (8 M) to obtain a final solution of 10 mM. Iodine (15 equiv, 34 mg mL^{-1} in MeOH) was added, which resulted in a dark red solution. The reaction was stirred for a maximum of 15 min at room temperature, followed by the addition of a 1,4-DTT solution (1 M) until the reaction mixture turned colorless. Then, a similar amount of 1,4-DTT was added again. This was followed by the addition of a 200 mM sodium carbonate solution to bring the pH to >7. The reaction was stirred for another 1 h and then purified by reversed-phase HPLC to obtain the Acm-deprotected peptide in fully reduced form. Standard oxidation was performed by dissolving a fully reduced compound at 1 mg mL^{-1} in Tris buffer (55 mM Tris·HCl, pH 8.0; 150 mM NaCl). The mixture was left at room temperature for a maximum of 3 days. The peak area of absorbance at 215 nm was used to quantify the product formation. When finished, a solution of 10% TFA was added to quench further oxidation.

Peptide array construct synthesis and affinity studies. Preparation of peptide–peptide arrays on polypropylene support was performed by using standard Fmoc chemistry. After side-chain deprotection by using TFA and scavengers, the peptide arrays were washed with an excess of Milli-Q water for 5–10 min and treated with a solution of scaffold (oS2-ONH_2 or oS2-CHO, 0.5 mM) in a mixture of MeCN/NH_4HCO_3 (1:3, 20 mM, pH 7.8) to afford the corresponding CLIPS-peptides. Oxime ligation was performed in 30 min by addition of a 1 mM solution of FSH β1 loop **7** or FSH β3 loop **5** in aniline/citric acid buffer (100 mM). The cards were washed again with an excess of Milli-Q water for 5–10 min and treated with a solution of iodine in MeOH (3.4 mg mL^{-1}) for 30 min, followed by washing with 1,4-DTT (1 M). Finally, the peptide arrays were washed with excess MeCN/H_2O (1:1) for 3–10 min and sonicated in disrupting buffer (1% SDS/0.1% BME in PBS, pH 7.2) at 70 °C for 30 min, followed by sonication in Milli-Q water for another 45 min.

Oxidation was performed prior to antibody binding studies by storing the cards in 0.1% NH_4HCO_3 buffer (pH 8.0) in open air for 1–2 days. Subsequent affinity studies were performed by pre-treatment with PBS for 30 min, followed by pre-coating with incubation buffer (PBS containing 5% ovalbumin, 5% horse serum, and 1% Tween-80) for 1 h. Then, the peptide arrays were incubated with mAbs 5828 or 6602 (diluted in incubation buffer to 1 ng mL^{-1}, 10 ng mL^{-1}, 100 ng mL,$^{-1}$ or 1 μg mL^{-1} solutions) for 1 h at 37 °C. After washing (3×10 min) with PBS/Tween-80 (0.05%), the peptides were incubated with peroxidase-labeled rabbit anti-mouse antibody for 1 h at 25 °C (1/1000; Dako, Glostrup, Denmark) and, after washing (3×10 min) with PBS/Tween-80 (0.05%), were subsequently incubated with the peroxidase substrate 2,2′-azino-di-3-ethylbenzthiazoline sulfonate (ABTS; 50 mg in 100 mL of 0.1 M citric acid-sodium phosphate buffer, pH 4.0, containing 20 μL 30% H_2O_2). After 1 h, the absorbance at 405 nm was measured by using a CCD camera (XC-77RR, Sony, Japan). Bound mAb was removed by sonication in disrupting buffer as described above. Oxidation was repeated to enable reuse of the peptide arrays.

Binding ELISA studies. Polystyrene 96-well plates (Greiner, Germany) were treated with 100 μL per well of 0.2% glutaric dialdehyde in phosphate buffer (0.1 M, pH 5) for 4 h at room temperature with shaking, followed by washing (3×10 min) with phosphate buffer (0.1 M, pH 8). Then, the wells were coated with 100 μL per well of a 1 μg mL^{-1} solution of hFSH/hCG or a 10 μg mL^{-1} solution of peptide mimic in phosphate buffer (0.1 M, pH 8) overnight at 37 °C. After washing with 1% Tween-80 (3x) and stabilizing in horse serum (4% in PBS/1% Tween-80/3% NaCl) for 30 min, the plates were incubated with antibody (6602/5828/3468/8G5) at various dilutions, starting with a standard antibody dilution of 3 μg mL^{-1} in the first well and threefold dilution steps in subsequent wells. Incubation was performed for 1 h at 37 °C, followed by washing with 1% Tween-80 (3x). Then, the plates were incubated with 100 μL per well of peroxidase-labeled rabbit-anti-ouse/sheep) serum (1/1000 dilution in 4% horse serum, see above) for 1 h at 25 °C, followed by washing with 1% Tween-80 (4×). Finally, the plates were incubated with a 0.5 μg mL^{-1} solution of ABTS (2,2′-azinedi(ethylbenzthiazolinesulfonate)) containing 0.006% H_2O_2 in citric acid/phosphate buffer (0.1 M each, pH 4). OD_{405} values were measured after standing for 45 min at room temperature in the dark. Anti-hFSH monoclonal antibodies were included in the analysis as positive controls.

Competition ELISA studies. The procedure was identical to that described for protein and peptide binding in ELISA (see above), with the only difference being that after coating with a 1 $\mu g\,mL^{-1}$ solution of hFSH/hCG or 10 $\mu g\,mL^{-1}$ solution of FSH-**Ia**, pre-incubation of antibody in the presence of hFSH/hCG/peptide mimic was carried out in a separate pre-incubation plate (1/3 dilution per step) for 30 min at 37 °C, followed by incubation for 1 h at 37 °C. The required mAb dilutions yielding an OD_{405} between 1.0 and 1.5 in binding ELISA were found to give optimal results as starting dilutions in the competition experiments.

Acknowledgements

This work was financially supported by The Netherlands Organization for Scientific Research (NWO) ECHO 700.57.017.

Keywords: constrained peptides · discontinuous epitope · multicyclic peptides · protein mimicry

[1] M. Z. Atassi, J. A. Smith, *Immunochemistry* **1978**, *15*, 609 – 610.
[2] U. Reineke, R. Sabat, R. Misselwitz, H. Welfle, H.-D. Volk, J. Schneider-Mergener, *Nat. Biotechnol.* **1999**, *17*, 271 – 275.
[3] R. Wyatt, P. D. Kwong, E. Desjardins, R. W. Sweet, J. Robinson, W. A. Hendrickson, J. G. Sodroski, *Nature* **1998**, *393*, 705 – 711.
[4] J. L. Teeling, W. J. M. Mackus, L. J. J. M. Wiegman, J. H. N. Van den Brakel, S. A. Beers, R. R. French, T. van Meerten, S. Ebeling, T. Vink, J. W. Slootstra, P. W. H. I. Parren, M. J. Glennie, J. G. J. Van de Winkel, *J. Immunol.* **2006**, *177*, 362 – 371.
[5] H. Chen, R. Luo, *J. Am. Chem. Soc.* **2007**, *129*, 2930 – 2937.
[6] H. S. Cho, K. Mason, K. X. Ramyar, A. M. Stanley, S. B. Gabelli, D. W. Denney, D. J. Leahy, *Nature* **2003**, *421*, 756 – 760.
[7] C. Wiesmann, G. Fuh, H. W. Christinger, C. Eigenbrot, J. A. Wells, A. M. deVos, *Cell* **1997**, *91*, 695 – 704.
[8] Y. Mukai, T. Nakamura, M. Yoshikawa, Y. Yoshioka, S. Tsunoda, S. Nakagawa, Y. Yamagata, Y. Tsutsumi, *Sci. Signal.* **2010**, *3*, ra83.
[9] M. H. V. Van Regenmortel, *Open Vaccine J.* **2009**, *2*, 33 – 44.
[10] P. Leinikki, M. Lehtinen, H. Hyoty, P. Parkkonen, M. L. Kantanen, J. Hakulinen, *Adv. Virus Res.* **1993**, *42*, 149 – 186.
[11] M. J. Gomara, I. Haro, *Curr. Med. Chem.* **2007**, *14*, 531 – 546.
[12] J. Villén, E. Borras, W. Schaaper, R. Meloen, M. Davila, E. Domingo, E. Giralt, D. Andreu, *ChemBioChem* **2002**, *3*, 175 – 182.
[13] L. D. Walensky, A. L. Kung, I. Escher, T. J. Malia, S. Barbuto, R. D. Wright, G. Wagner, G. L. Verdine, S. J. Korsmeyer, *Science* **2004**, *305*, 1466 – 1470.
[14] R. E. Moellering, M. Cornejo, T. N. Davis, C. Del Bianco, J. C. Aster, S. C. Blacklow, A. L. Kung, D. G. Gilliland, G. L. Verdine, J. E. Bradner, *Nature* **2009**, *462*, 182-U57.
[15] D. H. Appella, L. A. Christianson, D. A. Klein, D. R. Powell, X. L. Huang, J. J. Barchi, S. H. Gellman, *Nature* **1997**, *387*, 381 – 384.
[16] N. Srinivas, P. Jetter, B. J. Ueberbacher, M. Werneburg, K. Zerbe, J. Steinmann, B. Van der Meijden, F. Bernardini, A. Lederer, R. L. A. Dias, P. E. Misson, H. Henze, J. Zumbrunn, F. O. Gombert, D. Obrecht, P. Hunziker, S. Schauer, U. Ziegler, A. Kaech, L. Eberl, K. Riedel, S. J. DeMarco, J. A. Robinson, *Science* **2010**, *327*, 1010 – 1013.
[17] L. Martin, F. Stricher, D. Missé, F. Sironi, M. Pugnière, P. Barthe, R. Prado-Gotor, I. Freulon, X. Magne, C. Roumestand, A. Ménez, P. Lusso, F. Veas, C. Vita, *Nat. Biotechnol.* **2002**, *21*, 71 – 76.
[18] M. Mutter, S. Vuilleumier, *Angew. Chem. Int. Ed. Engl.* **1989**, *28*, 535 – 554; *Angew. Chem.* **1989**, *101*, 551 – 571.
[19] Y. Singh, G. T. Dolphin, J. Razkin, P. Dumy, *ChemBioChem* **2006**, *7*, 1298 – 1314.
[20] P. Dumy, I. M. Eggleston, S. Cervigni, U. Sila, X. Sun, M. Mutter, *Tetrahedron Lett.* **1995**, *36*, 1255 – 1258.
[21] J. F. Barry, A. P. Davis, M. N. Perez-Payas, M. R. J. Elsegood, R. F. W. Jackson, C. Gennari, U. Piarulli, M. Gude, *Tetrahedron Lett.* **1999**, *40*, 2849 – 2852.
[22] C. Geraci, G. M. L. Consoli, E. Galante, E. Bousquet, M. Pappalardo, A. Spadaro, *Bioconjugate Chem.* **2008**, *19*, 751 – 758.
[23] K. J. Jensen, J. Brask, *Biopolymers* **2005**, *80*, 747 – 761.
[24] R. Franke, C. Doll, V. Wray, J. Eichler, *Org. Biomol. Chem.* **2004**, *2*, 2847 – 2851.
[25] T. Opatz, R. M. J. Liskamp, *Org. Lett.* **2001**, *3*, 3499 – 3502.
[26] Y. Singh, M. J. Stoermer, A. J. Lucke, T. Guthrie, D. P. Fairlie, *J. Am. Chem. Soc.* **2005**, *127*, 6563 – 6572.
[27] P. S. Ghosh, A. D. Hamilton, *J. Am. Chem. Soc.* **2012**, *134*, 13208 – 13211.
[28] I. Lasters, J. Desmet, M. Henderikx, A. Wehnert, G. Meersseman, WO2012093172A1.
[29] K. M. Fox, J. A. Dias, P. Van Roey, *Mol. Endocrinol.* **2001**, *15*, 378 – 389.
[30] A. J. Lapthorn, D. C. Harris, A. Littlejohn, J. W. Lustbader, R. E. Canfield, K. J. Machin, F. J. Morgan, N. W. Isaacs, *Nature* **1994**, *369*, 455 – 461.
[31] J. G. Pierce, T. F. Parsons, *Annu. Rev. Biochem.* **1981**, *50*, 465 – 495.
[32] P. Timmerman, E. Van Dijk, W. Puijk, W. Schaaper, J. Slootstra, S. J. Carlisle, J. Coley, S. Eida, M. Gani, T. Hunt, P. Perry, G. Piron, R. H. Meloen, *Mol. Diversity* **2004**, *8*, 61 – 77.
[33] M. Tegoni, S. Spinelli, M. Verhoeyen, P. Davis, C. Cambillau, *J. Mol. Biol.* **1999**, *289*, 1375 – 1385.
[34] P. Timmerman, J. Beld, W. C. Puijk, R. H. Meloen, *ChemBioChem* **2005**, *6*, 821.
[35] A. Dirksen, T. M. Hackeng, P. E. Dawson, *Angew. Chem. Int. Ed.* **2006**, *45*, 7581 – 7584; *Angew. Chem.* **2006**, *118*, 7743 – 7746.
[36] B. D. Larsen, A. Holm, *J. Pept. Res.* **1998**, *52*, 470 – 476.
[37] C. R. Gregor, E. Cerasoli, J. Schouten, J. Ravi, J. Slootstra, A. Horgan, G. J. Martyna, M. G. Ryadnov, P. Davis, J. Crain, *J. Biol. Chem.* **2011**, *286*, 25016 – 25026.
[38] H. M. Geysen, R. H. Meloen, S. J. Bartelings, *Proc. Natl. Acad. Sci. USA* **1984**, *81*, 3998 – 4002.
[39] P. Timmerman, W. C. Puijk, R. H. Meloen, *J. Mol. Recognit.* **2007**, *20*, 283 – 299.
[40] P. Timmerman, R. Barderas, J. Desmet, D. Altschuh, S. Shochat, M. J. Hollestelle, J. W. M. Hoppener, A. Monasterio, J. I. Casal, R. H. Meloen, *J. Biol. Chem.* **2009**, *284*, 34126 – 34134.
[41] L. E. J. Smeenk, N. Dailly, H. Hiemstra, J. H. van Maarseveen, P. Timmerman, *Org. Lett.* **2012**, *14*, 1194 – 1197.
[42] B. Kamber, A. Hartmann, K. Eisler, B. Riniker, H. Rink, P. Sieber, W. Rittel, *Helv. Chim. Acta* **1980**, *63*, 899 – 915.
[43] C. Heinis, T. Rutherford, S. Freund, G. Winter, *Nat. Chem. Biol.* **2009**, *5*, 502 – 507.

Received: September 17, 2014
Published online on December 2, 2014